JOURNAL OF GEOPHYSICAL RESEARCH: OCEANS, VOL. 118, 5669–5675, doi:10.1002/jgrc.20407, 2013

The control of the Southern Hemisphere Westerlies on the position of the Subtropical Front

Agatha M. De Boer,[1,2] Robert M. Graham,[1,2] Matthew D. Thomas,[3] and Karen E. Kohfeld[4]

Received 2 May 2013; revised 12 August 2013; accepted 20 September 2013; published 22 October 2013.

[1] In recent years the latitudinal position of the Subtropical Front (STF) has emerged as a key parameter in the global climate. A poleward positioned front is thought to allow a greater salt flux from the Indian to the Atlantic Ocean and so drive a stronger Atlantic Meridional Overturning Circulation. Here the common view that the STF aligns with the zero wind stress curl (WSC) is challenged. Based on the STF climatologies of Orsi et al. (1995), Belkin and Gordon (1996), Graham and De Boer (2013), and on satellite scatterometry winds, we find that the zero WSC contour lies on average ∼10°, ∼8°, and ∼5° poleward of the front for the three climatologies, respectively. The circulation in the region between the Subtropical Gyres and the zero WSC contour is not forced by the WSC but rather by the strong bottom pressure torque that is a result of the interaction of the Antarctic Circumpolar Current with the ocean floor topography. The actual control of the position of the STF is crucially dependent on whether the front is regarded as simply a surface water mass boundary or a dynamical front. For the Agulhas Leakage problem, the southern boundary of the so-called Super Gyre may be the most relevant property but this cannot easily be identified in observations.

Citation: De Boer, A. M., R. M. Graham, M. D. Thomas, and K. E. Kohfeld (2013), The control of the Southern Hemisphere Westerlies on the position of the Subtropical Front, *J. Geophys. Res. Oceans*, *118*, 5669–5675, doi:10.1002/jgrc.20407.

1. Introduction

[2] The latitudinal position of the STF in the Southern Ocean has been related to the magnitude of water transport from the Indian Ocean to the Atlantic Ocean. This leakage, mostly in the form of Agulhas Rings, provides a salt flux to the Atlantic that may strengthen and stabilize the Atlantic Meridional Overturning Circulation [*Bard and Rickaby*, 2009; *Beal et al*., 2011; *Weijer et al*., 2001, 2002]. A wind-induced change in the position of the STF has therefore been suggested to indicate altered Indian-Atlantic salt exchange that could be strongly influence the nature of climate transitions during the Quaternary [*Bard and Rickaby*, 2009; *Peeters et al*., 2004] and current Anthropocene [*Beal et al*., 2011; *Biastoch et al*., 2009]. In these studies, the position of the STF is usually linked to the latitude of zero WSC so that a latitudinal movement of the wind field will cause an associated shift in the front [*Biastoch et al*., 2009; *de Ruijter et al*., 1999; *Dencausse et al*., 2011; *Peeters et al*., 2004; *Zharkov and Nof*, 2008].

[3] The truism that the STF position shifts meridionally with a shift in the overlying wind field is also often applied to infer changes in Southern Hemisphere westerly winds during the Last Glacial Maximum (LGM, ∼19,000–230,000 calendar years ago) from proxies for the position of the front (see *Kohfeld et al*. [2013] for a comprehensive review). A northward shift in the westerly winds has been proposed to reduce upwelling and outgassing of CO_2 to the atmosphere [*Toggweiler et al*., 2006]. Despite that both the ideas that the LGM winds have shifted northward and that it may have reduced atmospheric CO_2 have been questioned [*d'Orgeville et al*., 2010; *Lauderdale et al*., 2013; *Menviel et al*., 2008; *Sime et al*., 2013; *Tschumi et al*., 2008], the theory remains a strong contender for explaining the glacial drawdown of CO_2.

[4] The idea that the STF corresponds to the zero WSC is based on a frequent definition of the STF as the boundary between the Subtropical Gyre and the ACC [*Stramma*, 1992], and a simple theory that relates the poleward boundary of the Subtropical Gyres to the location of the zero WSC [*de Ruijter*, 1982]. This theory solves the vertically integrated vorticity equation of *Munk* [1950] for the southern Atlantic-Indian ocean region. The equations include planetary vorticity and vorticity from winds and lateral eddy viscosity but does not include the contribution of

Companion paper to *Graham and De Boer* [2013] doi:10.1002/jgrc.20408.

[1]Department of Geological Sciences, Stockholm University, Stockholm, Sweden.
[2]Bolin Centre for Climate Research, Stockholm University, Stockholm, Sweden.
[3]Laboratoire de Physique des Oceans, Ifremer, Plouzane, France.
[4]School of Resource and Environmental Management, Simon Frasier University, Burnaby, British Columbia, Canada.

Corresponding author: A. M. De Boer, Department of Geological Sciences, Stockholm University, Stockholm SE-106 91, Sweden. (agatha.deboer@geo.su.se)

2169-9275/13/10.1002/jgrc.20407

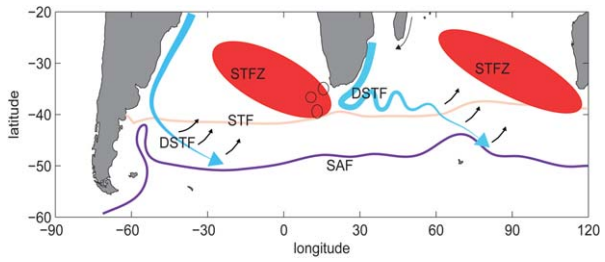

Figure 1. Position of new Dynamical STF (DSTF, blue arrows) from *Graham and De Boer* [2013] in relation to the traditional STF water mass boundary (peach). The DSTF in the western side of basins has strong SSH gradients, SST gradients, and currents associated with it while Subtropical Frontal Zones (red ovals) at the eastern side of the basins have weak fronts with no transport. As indicated by the direction of the arrows, the DSTF traverses to the southeast to join the Sub-Antarctic Front (SAF, purple line) so that the DSTF and STFZ are disconnected.

bottom pressure torque. Hence, similar to *Munk* [1950] the boundaries of the gyre correspond to the zero WSC. The STF is also sometimes referred to as the Subtropical Convergence Zone which stems from its alternative perception as a feature coinciding with the maximum wind stress curl where the convergence is maximum [*Peterson and Stramma*, 1991; *Stramma*, 1992; *Zharkov and Nof*, 2008]. The simple theory that relates the position of the STF to the zero WSC is powerful and has strong implications for our interpretations of climate responses to changes in the position of westerly winds. However, its general applicability is hampered by our poor understanding of what the front is and how it is controlled.

[5] In a companion paper, *Graham and De Boer* [2013] review the currently available definitions and climatologies of the STF. They also provide a new Dynamical STF climatology based on maxima in satellite sea surface height (SSH) gradients, which have been verified as a measure of strong currents [*Graham et al*., 2012]. The relationship between the traditional STF water mass boundary and the Dynamical STF is illustrated in Figure 1. The Dynamical STF corresponds to the separated Western Boundary Currents in each basin and form the southern boundary of the Subtropical Gyres on the western sides of the gyres (on the eastern side there are no strong currents). The motivation for distinguishing between the water mass boundary STF and the Dynamical STF is that they are not constrained in the same way by the underlying bathymetry and are expected to respond very differently to changes in wind stress and water mass properties. In this paper, we determine the relation between the WSC and both the traditional STF and the new Dynamical STF. The comparison is done from observations and then a high resolution coupled climate model is used to investigate the theory that relates the WSC and STF.

2. Methods

2.1. Data Comparison

[6] The wind stress climatology used in the comparison is derived from NASA QuickSCAT satellite wind stress data [*Risien and Chelton*, 2008] which cover the period of September 1999 to August 2009. The wind stress data are time averaged over the full period before the curl is calculated. The resulting WSC field is then smoothed over 6° latitude and 10° longitude which amounts to smoothing of approximately 650 km in each direction at 55°S (Figure 2). The three climatologies used for the position of the STF are that of *Orsi et al*. [1995], *Belkin and Gordon* [1996], and *Graham and De Boer* [2013]. The first two climatologies [*Orsi et al*., 1995; *Belkin and Gordon*, 1996] are based on a synthesis of ship-based hydrographic data and define the front as the boundary between the Subtropical and Sub-Antarctic surface water masses. The third [*Graham and De Boer*, 2013] relates specifically to the strong currents at the STF water mass boundary. The data from which the dynamic STF climatology was derived cover the same 10 year period as the satellite wind stress data used in this study so that the fronts and winds from these products are consistent with each other.

2.2. Model Description and Validation

[7] We use the HiGEM1.1 model that is a fully coupled ocean-atmosphere model developed at the UK Met Office and based on the earlier lower resolution model HadGEM1

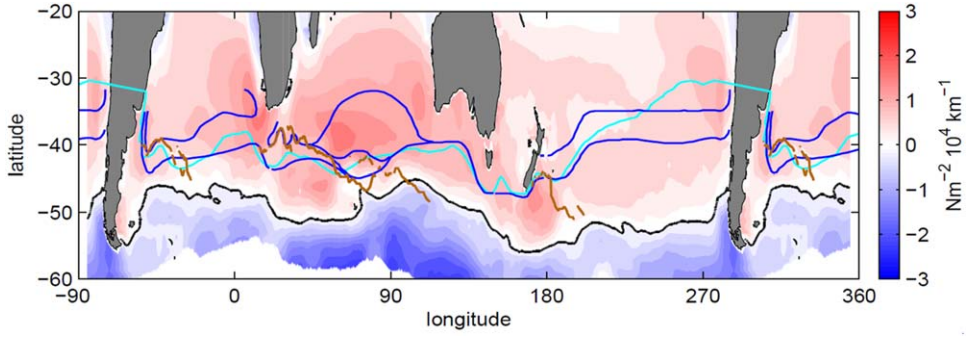

Figure 2. Correspondence between the satellite-derived zero WSC (solid black line) and the STF. The STF climatologies are from *Orsi et al*. [1995, light blue line], *Belkin and Gordon* [1996, dark blue lines], and the Dynamical STF of *Graham and De Boer* [2013, brown line]. Background colors indicate the WSC from QuickScat satellite scatterometry and the white areas at the bottom of the figure is due to lack of data.

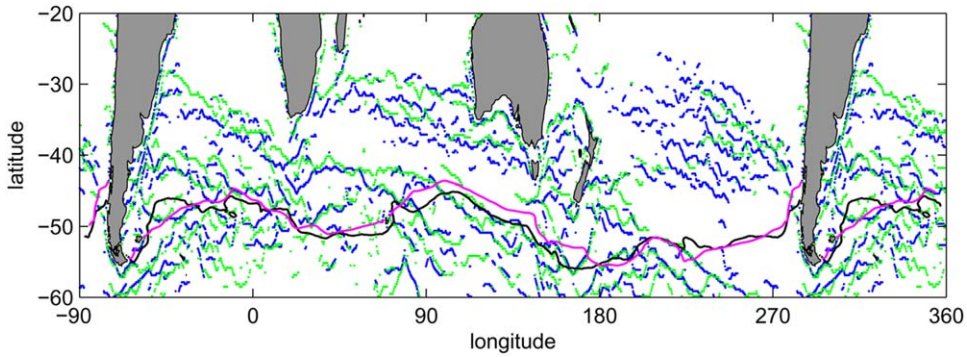

Figure 3. Fronts identified in maxima in SST gradients from satellite data (blue) and HiGEM (green). Also indicated are the zero WSC contour from satellite (black line) and HiGEM (pink) data.

[*Roberts et al*., 2009; *Shaffrey et al*., 2009]. The horizontal resolution in the atmosphere is 0.83° latitude × 1.25° longitude with 38 levels in the vertical reaching from the surface to 39 km. The horizontal resolution in the ocean and sea ice components is a 1/3° × 1/3° in both directions. In the ocean there are 40 unevenly spaced levels in the vertical varying from about 10 m at the surface to 300 m at the bottom which is at 5500 m. At this resolution, a grid box at 45°S is 37 km × 26 km in the meridional and zonal directions, respectively, which is sufficient to resolve the Southern Ocean fronts and partially represent eddies. The isopycnal formulation of *Griffies* [1998] is used to mix tracers laterally. No Gent-McWilliams parameterization is used [*Gent and McWilliams*, 1990]. In this study, we make use of a 150 year control run in which greenhouse gas concentrations have been kept constant at present day values (i.e., CO_2 concentration is 345 ppm). All the analysis presented here is from fields averaged over the final 30 years of model output.

[8] The HiGEM model has already been validated to study Southern Ocean fronts [*Graham et al*., 2012]. Further justification for its use is provided by its excellent ability to reproduce the maxima in sea surface temperature gradients associated with frontal features observed from satellite data (Figure 3). Within the Southern Ocean itself, the position of the frontal features in the model and observations are strikingly similar. Further north, in the Subtropical Gyres, the location of SST fronts in the model and observations do not correspond as closely, but there are no obvious differences in the structure of the frontal features, i.e., their spacing, length, or angle. This region of SST gradient fronts north of the Antarctic Circumpolar Current and on the eastern side of the Subtropical Gyres has been coined the Subtropical Frontal Zone [*Graham and De Boer*, 2013]. Unlike the fronts within the Southern Ocean that are deep and have negligible seasonal cycles, the fronts in the Subtropical Frontal Zone are shallow and more seasonally variable [*Graham and De Boer*, 2013]. It is therefore not surprising that the model captures the position of the fronts in the Southern Ocean better than those in the Subtropical Frontal Zone.

3. The Subtropical Front, Wind Stress Curl and Vorticity

[9] We find that the zero WSC contour lies consistently poleward of the STF for all definitions of the front at almost all longitudes (Figure 2). The mean distances between the front and the zero WSC are 10°, 8°, and 5° for the *Orsi et al*. [1995], *Belkin and Gordon* [1996], and *Graham and De Boer* [2013] climatologies, respectively. (At longitudes where the STF for any climatology is split into more than one front, the branch that is closest to the zero WSC contour is used in the calculation.) The STF is also not aligned with the maximum WSC (Figure 2, dark red regions).

[10] To understand why the STF does not correspond to the zero WSC, it is useful to briefly revisit the theory on which the assumption is based. The balance for the full depth-integrated vorticity, also called the barotropic vorticity, can be written as [*Hughes and de Cuevas*, 2001; *Lu and Stammer*, 2004; *Rintoul et al*., 2001]

$$\rho_0 \beta \mathrm{V} = \hat{k} \cdot (\nabla \times \tau) - \nabla p_\mathrm{b} \times \nabla H + \delta. \tag{1}$$

[11] The first term represents the change in planetary vorticity and is the product of the full depth-integrated meridional velocity V, a constant reference density ρ_0, and the meridional gradient of the Coriolis parameter $\beta = \mathrm{d}f/\mathrm{d}y$. The second term is the input of vorticity by the wind stress, τ, where ∇ is the horizontal gradient operator and $\hat{k}$ is the vertical unit vector pointing upward. The third term, in which p_b is the bottom pressure and H is the ocean depth, describes the source of vorticity created by the bottom pressure torque, or in other words, the vorticity created by the interaction of the horizontal flow with topography. The final term δ represents the contribution of all other sources (i.e., lateral friction and nonlinear advection).

[12] If the vorticity equation is depth integrated to a fix depth, h, then equation (1) would be slightly revised to

$$P_0 \beta \mathrm{V} = \hat{k} \cdot (\nabla \times \tau) - f w_h + \ \delta, \tag{2}$$

where w_h is the vertical velocity at depth h and depth integrated terms are only integrated from the surface to h. (Note that the residual here includes the small contribution from the curl of the stress at h.) In the subtropics, away from western boundary currents, the third and fourth terms in equation (2) are usually negligible (when smoothed over about 5°) which means that the upper layer meridional flow is determined by the WSC alone [*Wunsch*, 2011]. In such a scenario, the ocean is said to be in Sverdrup balance and the meridional flow vanishes where $\nabla \times \tau = 0$. Therefore, if we define the STF as the southern boundary of the Subtropical Gyre, which is where the meridional flow is zero,

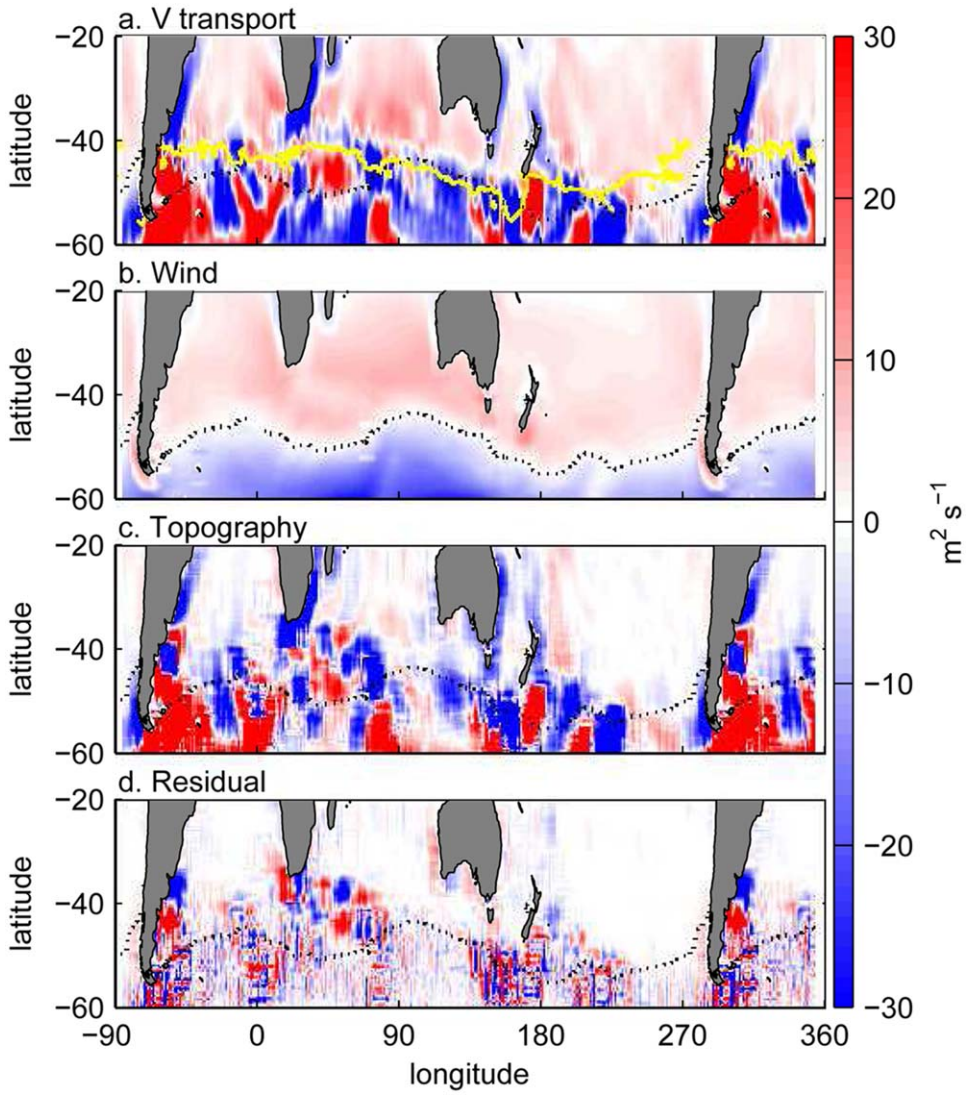

Figure 4. Terms in the vorticity balance in equation (1) calculated from HiGEM model data and divided by $\rho_0\beta$ to transform to units of depth integrated transport. The change in planetary vorticity due to (a) meridional transport (b) is balanced by the source of vorticity from the wind and (c) the bottom pressure torque. (d) The residual indicates the deviation from linear vorticity balance. The black line is the zero WSC contour and the yellow line shows the position of the zero barotropic streamfunction. Units are $m^2\ s^{-1}$.

the STF would correspond to the zero WSC. The crucial question for the theory to apply is whether the Southern Hemisphere subtropical oceans are in Sverdrup balance from the subtropics extending poleward to the latitude of zero WSC.

[13] We analyze the barotropic vorticity balance in the Southern Ocean in 30 year averaged output from HiGEM. Each term in equation (1) is calculated from HiGEM output and smoothed to the same degree as the wind stress observations (6° latitude × 10° longitude). Their magnitudes (divided by $\rho_0\beta$ to represent transport) are presented in Figure 4. The terms in Figures 4b–4d add up to the transport in Figure 4a. As one might expect, in the Subtropical Gyres, the transport (Figure 4a) corresponds well with the wind stress curl (Figure 4b). South of the gyres' boundary (Figure 4a, yellow line), the transport is more strongly controlled by the bottom pressure torque (Figure 4c). The residual term (δ), which is related to the lateral friction and nonlinear advection, is not very important in driving the transport at these spatial scales of smoothing, except perhaps near the Drake Passage (Figure 4d). However, similar to what other authors have found [*Hughes and de Cuevas*, 2001] the contribution of lateral friction and nonlinear advection is substantial at smaller scales (Figure 5d). These analyses show that large-scale meridional transport in the Southern Ocean is primarily controlled by the bottom pressure torque, and that the control of the wind only becomes significant in the Subtropical Gyres. The same analysis was repeated for equation (2), integrated to 2 km depth, and produced a very similar picture to Figure 4 (not shown).

[14] The dominance of bottom pressure torque in the vorticity balance of the Southern Ocean is not a new result [*Olbers and Visbeck*, 2005; *Rintoul et al*., 2001; *Wells and De Cuevas*, 1995]. However, as noted above, there appears to be a common misconception that the zero WSC contour lies north of this topographically controlled region and

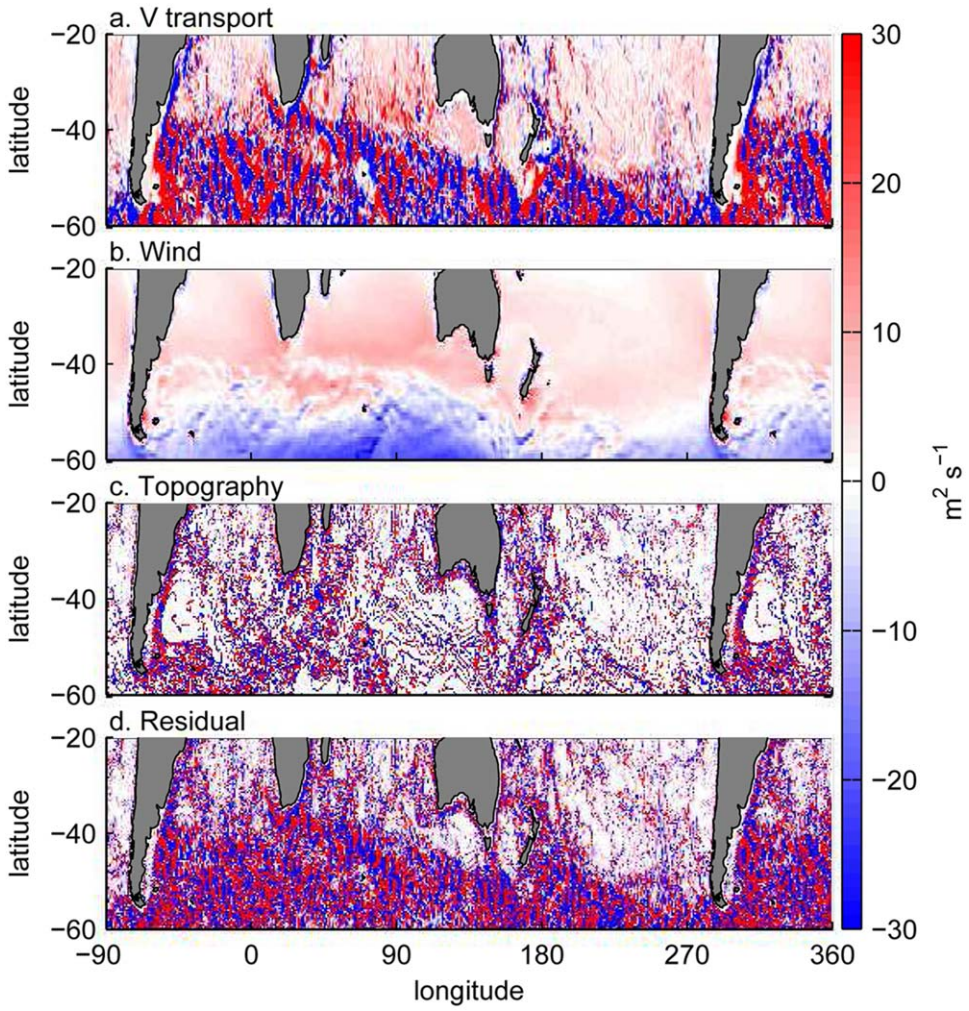

Figure 5. Same as in Figure 3 but the terms are unsmoothed.

corresponds closely to the southern boundary of the Subtropical Gyres. In reality, the zero WSC contour (Figure 4, black line) lies firmly in the Southern Ocean, up to 10° south of the Subtropical Gyres at places. The Dynamical STF marks the southern boundary of the Subtropical Gyres, which sits just north of the super gyre boundary defined by the zero barotropic streamfunction (Figure 6). Thus, the evidence laid out above that the zero WSC does not control the southern boundary of the gyres applies equally to the inability of the WSC to directly control the position of the Dynamical STF. Of course, this does not mean that the position of the Dynamical STF or southern gyre boundary is not affected by the winds in the Southern Hemisphere but more work is needed to investigate the relationship.

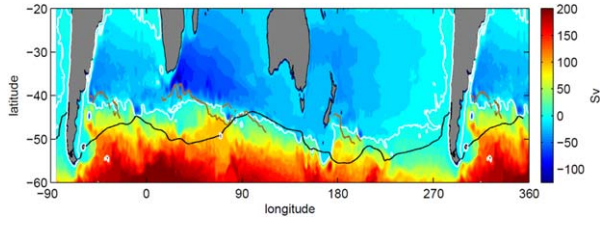

Figure 6. Barotropic streamfunction in HiGEM. The white contour outlines the zero streamfunction which is the boundary between the Subtropical Gyres and the Southern Ocean and often used as a definition of the STF. The zero WSC contours are shown in black, and brown lines indicate the Dynamical STF according to *Graham and De Boer* [2013] climatology.

4. Discussion

[15] We have used satellite observations of the wind field to show that neither the STF defined as a surface water mass boundary nor the Dynamical STF related to currents corresponds with the position of the zero WSC. Seemingly contrary to this statement, there is in fact a narrow band of zero WSC right above the Dynamical STF (Figure 5b, also evident in unsmoothed satellite WSC data). However, this is just a local band and does not delineate the zone of positive WSC from that of negative WSC, i.e., south of this band the WSC increases again. The flattening of the wind field is related to the feedback of the sea surface temperature gradients across the front on the overlying winds. Specifically, over colder water the surface layer of the atmosphere is more stable. Therefore, wind speeds decrease more rapidly toward the ocean surface compared to over

the warmer water [*Chelton et al*., 2004; *Small et al*., 2008]. The wind stress is greater over the warm water on the northern side of the front and weaker on the southern side of the front where the water is colder. This creates a positive meridional gradient anomaly in the zonal wind stress over the front, which is opposite to the background negative gradient, and thus results in a local zero in the wind stress curl (Figure 5b).

[16] To answer the question of what sets the position of the STF (if not the zero WSC), one would first have to state whether the question pertains to the STF water mass boundary (e.g., as defined by *Orsi et al*. [1995] or *Belkin and Gordon* [1996]), the southern boundary of the so-called Atlantic-Indian Ocean Supergyre, or the Dynamical STF of *Graham and De Boer* [2013]. *Graham and De Boer* [2013] showed that the STF water mass boundary does not respond to the southern boundaries of the Subtropical Gyres or the Super Gyre. The Dynamical STF follows the southern boundary of the Subtropical Gyres but only on the western side of basins. The southern boundary of the Super Gyre lies to the south for the individuals Subtropical Gyres but it is not easily identified in observations as a front or water mass boundary. Its responds to winds would therefore be difficult to observe in modern or paleo-data.

[17] The southern boundary of the Atlantic-Indian Super Gyre lies on the northern border of the ACC and so it is reasonable to assume that its position is related to the northward extent of the ACC. It should also be related to the size of the Subtropical Gyres. An expansion of the Subtropical Gyres due to a southward shift in the westerly winds has been put forth to explain southward movement of the STF and a contraction of the ACC in high resolution climate change simulations [*Graham et al*., 2012; *Wang et al*., 2011]. It stands to reason that the boundary of the Subtropical Gyres will always lie as far south and as close to the zero WSC as the ACC will allow it to be. Within the ACC, the bottom pressure torque will override the control of the wind in the vorticity balance. In the Atlantic, after the ACC exits the Drake Passage, the current is deflected sharply northward at the East Scotia Ridge, and this deflection has been loosely associated with the wind stress field [*Allison et al*., 2010; *Marshall*, 1995; *Rintoul et al*., 2001]. The path of the rest of the ACC is often attributed to the control of the topography [*Graham et al*., 2012; *Marshall*, 1995]. Support for the topographic control of the fronts in the Southern Ocean is provided by the strikingly similar positions of the Southern Ocean frontal features in the independent fully coupled model output and satellite data (Figure 3), the small seasonal cycle of the fronts within the ACC (see *Graham and De Boer* [2013], Figure 8), and the small change in position of fronts in response to a 100 year future warming simulation [*Graham et al*., 2012].

[18] Another interesting aspect of the problem regarding what sets the position of the STF is that the bottom pressure torque and meridional transport are not only related within the ACC but are also highly correlated at the Dynamical STF in the Indian Ocean north of the ACC (see blue band north of zero streamfunction in Figures 4a and 4c). The upper ocean is, therefore, not in Sverdrup balance there at these large scales. It is likely that the strong eastward current associated with the Dynamical STF is countering the westward propagating baroclinic Rossby waves. These Rossby waves usually confine the flow to the surface in the Subtropical Gyres [*Anderson and Killworth*, 1977]. At higher latitudes, the baroclinic Rossby waves speed is slower and can more easily be countered by the mean flow [*Hughes and de Cuevas*, 2001]. If the diminishing Rossby wave speed toward high latitudes was the only factor determining where the wind control breaks down we would expect to see a more zonal pattern in the boundary between wind control and topographic control of the vorticity. However, the wind control stretches much further south in the Pacific Ocean compared with the Indian and Atlantic Oceans (Figure 4).

[19] The Dynamical STF is in essence an extension of the separated western boundary currents of the Subtropical Gyres in the Atlantic and Indian Oceans (Figure 1). In the Indian Ocean, this is equivalent to the Agulhas Return Current. The latitude of Agulhas Current retroflection and its influence on the Agulhas Leakage is still a matter of intense research [*Le Bars et al*., 2012; *Nof et al*., 2011; *van Sebille et al*., 2009]. However, it is clear that the current is retroflecting because the African continent ends and it will never reach as far south as the current day zero WSC. Moreover, if the Agulhas Return Current would ever correspond to the zero WSC in glacial times, the zero WSC would have to shift about 10° north and the Agulhas Return Current remain in the same position.

5. Summary

[20] We have shown that the assumed correspondence between the zero WSC and the STF does not exist. The lack of alignment between the STF, defined as the southern boundary of the Subtropical Gyres, and the zero WSC seems to be at least partly a consequence of the ACC whose northern boundary lies north of the position of the zero WSC. Within the ACC, the meridional flow is dominated by the bottom pressure torque at scales larger than ∼5° and therefore the direct control of the wind stress curl breaks down. The bottom pressure torque is also important just north of the ACC within the Dynamical STF where the strong eastward current counters the slow first mode baroclinic Rossby waves that otherwise sets the upper ocean in Sverdrup balance. What determines the position of the Dynamical STF in the Indian Ocean (i.e., the Agulhas Return Current), and the Atlantic and Pacific Oceans, is still a question of debate. However, the position of the Dynamical STF does seem more sensitive to changes in the Southern Hemispheric Westerlies than fronts within the Antarctic Circumpolar Current [*Graham et al*., 2012] and its strength is also correlated with that of the Westerlies [*Durgadoo et al*., 2013].

[21] There is support in the literature for a meridional shift in the STF surface water mass boundary and plankton assemblage at glacial intervals [*Kohfeld et al*., 2013; *Peeters et al*., 2004] and this has been related to a shift in the wind. This paper cautions against these results being over-interpreted as direct evidence that the southward extent of the Southern Hemisphere Subtropical Gyres is set by the latitude of zero WSC. To utilize the wealth of available paleo-data regarding Southern Ocean water masses more effectively, it would be useful to have a better understanding of what controls the meridional position of water masses. This study also motivates for a more detailed analysis of how the strength, position, and meridional structure

of the westerly winds control the Subtropical Gyre extent in the Southern Hemisphere, the western boundary current separation in the Atlantic and Indian Ocean, and the position of the ACC and how all these are related. An improved understanding of these processes will facilitate the interpretation of paleo-proxies for water mass properties and may help to predict what a warming induced southward shift in the westerly winds may imply for Agulhas Leakage and the Meridional Overturning Circulation.

[22] **Acknowledgments.** The model output was kindly provided by David Stevens. The model was developed from the Met Office Hadley Centre Model by the UK High-Resolution Modelling (HiGEM) Project and the UK Japan Climate Collaboration (UJCC). HiGEM is supported by a NERC High Resolution Climate Modelling Grant (R8/H12/123). UJCC was supported by the Foreign and Commonwealth Office Global Opportunities Fund, and jointly funded by NERC and the DECC/Defra Met Office Hadley Centre Climate Programme (GA01101). The work of Professor Pier Luigi Vidale and Dr. Malcolm Roberts in leading the effort in Japan is particularly valued.

References

Allison, L. C., H. L. Johnson, D. P. Marshall, and D. R. Munday (2010), Where do winds drive the Antarctic Circumpolar Current?, *Geophys. Res. Lett.*, *37*, L12605, doi:10.1029/2010GL043355.

Anderson, D. L. T., and P. D. Killworth (1977), Spin-up of a stratified ocean, with topography, *Deep Sea Res.*, *24*(8), 709–732.

Bard, E., and R. E. M. Rickaby (2009), Migration of the subtropical front as a modulator of glacial climate, *Nature*, *460*(7253), 380–383.

Beal, L. M., W. P. M. De Ruijter, A. Biastoch, and R. Zahn (2011), On the role of the Agulhas system in ocean circulation and climate, *Nature*, *472*(7344), 429–436.

Belkin, I. M., and A. L. Gordon (1996), Southern Ocean fronts from the Greenwich meridian to Tasmania, *J. Geophys. Res.*, *101*(C2), 3675–3696.

Biastoch, A., C. W. Boning, F. U. Schwarzkopf, and J. R. E. Lutjeharms (2009), Increase in Agulhas leakage due to poleward shift of Southern Hemisphere Westerlies, *Nature*, *462*(7272), 495–498.

Chelton, D. B., M. G. Schlax, M. H. Freilich, and R. F. Milliff (2004), Satellite measurements reveal persistent small-scale features in ocean winds, *Science*, *303*(5660), 978–983.

d'Orgeville, M., W. P. Sijp, M. H. England, and K. J. Meissner (2010), On the control of glacial-interglacial atmospheric CO_2 variations by the Southern Hemisphere Westerlies, *Geophys. Res. Lett.*, *37*, L21703, doi:10.1029/2010GL045261.

de Ruijter, W. P. M. (1982), Asymptotic analysis of the Agulhas and Brazil current systems, *J. Phys. Oceanogr.*, *12*(4), 361–373.

de Ruijter, W. P. M., A. Biastoch, S. S. Drijfhout, J. R. E. Lutjeharms, R. P. Matano, T. Pichevin, P. J. van Leeuwen, and W. Weijer (1999), Indian-Atlantic interocean exchange: Dynamics, estimation and impact, *J. Geophys. Res.*, *104*(C9), 20,885–20,910.

Dencausse, G., M. Arhan, and S. Speich (2011), Is there a continuous Subtropical Front south of Africa?, *J. Geophys. Res.*, *116*, C02027, doi:10.1029/2010JC006587.

Durgadoo, J. V., B. R. Loveday, C. J. C. Reason, P. Penven, and A. Biastoch (2013), Agulhas leakage predominantly responds to the Southern Hemisphere Westerlies, *J. Phys. Oceanogr.*, *43*, 2113–2131, doi:10.1175/JPO-D-13-047.1.

Gent, P. R., and J. C. McWilliams (1990), Isopycnal mixing in ocean circulation models, *J. Phys. Oceanogr.*, *20*(1), 150–155.

Graham, R. M., and A. M. De Boer (2013), The dynamical subtropical front, *J. Geophys. Res. Oceans*, *118*, doi:10.1002/jgrc.20408.

Graham, R. M., A. M. De Boer, K. J. Heywood, M. R. Chapman, and D. P. Stevens (2012), Southern Ocean fronts: Controlled by wind or topography?, *J. Geophys. Res.*, *117*, C08018, doi:10.1029/2012JC007887.

Griffies, S. M. (1998), The Gent-McWilliams skew flux, *J. Phys. Oceanogr.*, *28*(5), 831–841.

Hughes, C. W., and B. A. de Cuevas (2001), Why western boundary currents in realistic oceans are inviscid: A link between form stress and bottom pressure torques, *J. Phys. Oceanogr.*, *31*(10), 2871–2885.

Kohfeld, K. E., R. M. Graham, A. M. de Boer, L. C. Sime, E. W. Wolff, C. Le Quéré, and L. Bopp (2013), Southern Hemisphere westerly wind changes during the last glacial maximum: Paleo-data synthesis, *Quat. Sci. Rev.*, *68*, 76–95.

Lauderdale, J., A. N. Garabato, K. C. Oliver, M. Follows, and R. Williams (2013), Wind-driven changes in Southern Ocean residual circulation, ocean carbon reservoirs and atmospheric CO_2, *Clim. Dyn.*, *41*, 1–20.

Le Bars, D., W. P. M. De Ruijter, and H. A. Dijkstra (2012), A new regime of the Agulhas current retroflection: Turbulent choking of Indian–Atlantic leakage, *J. Phys. Oceanogr.*, *42*(7), 1158–1172.

Lu, Y., and D. Stammer (2004), Vorticity balance in coarse-resolution global ocean simulations, *J. Phys. Oceanogr.*, *34*(3), 605–622.

Marshall, D. (1995), Topographic steering of the Antarctic Circumpolar Current, *J. Phys. Oceanogr.*, *25*(7), 1636–1650.

Menviel, L., A. Timmermann, A. Mouchet, and O. Timm (2008), Climate and marine carbon cycle response to changes in the strength of the Southern Hemispheric Westerlies, *Paleoceanography*, *23*, PA4201, doi:10.1029/2008PA001604.

Munk, W. H. (1950), On the wind-driven ocean circulation, *J. Meteorol.*, *7*(2), 80–93.

Nof, D., V. Zharkov, J. Ortiz, N. Paldor, W. Arruda, and E. Chassignet (2011), The arrested Agulhas retroflection, *J. Mar. Res.*, *69*(4–6), 659–691.

Olbers, D., and M. Visbeck (2005), A model of the zonally averaged stratification and overturning in the Southern Ocean, *J. Phys. Oceanogr.*, *35*(7), 1190–1205.

Orsi, A. H., T. Whitworth III, and W. D. Nowlin Jr. (1995), On the meridional extent and fronts of the Antarctic Circumpolar Current, *Deep Sea Res., Part I*, *42*(5), 641–673.

Peeters, F. J. C., R. Acheson, G.-J. A. Brummer, W. P. M. de Ruijter, R. R. Schneider, G. M. Ganssen, E. Ufkes, and D. Kroon (2004), Vigorous exchange between the Indian and Atlantic oceans at the end of the past five glacial periods, *Nature*, *430*(7000), 661–665.

Peterson, R. G., and L. Stramma (1991), Upper-level circulation in the South Atlantic Ocean, *Prog. Oceanogr.*, *26*(1), 1–73.

Rintoul, S. R., C. W. Hughes, and D. Olbers (2001), The Antarctic Circumpolar Current system, in *International Geophysics*, edited by J. C. G. Siedler and G. John, pp. 271–302, Academic, San Diego, Calif.

Risien, C. M., and D. B. Chelton (2008), A global climatology of surface wind and wind stress fields from eight years of QuikSCAT scatterometer data, *J. Phys. Oceanogr.*, *38*(11), 2379–2413.

Roberts, M. J., et al. (2009), Impact of resolution on the tropical pacific circulation in a matrix of coupled models, *J. Clim.*, *22*(10), 2541–2556.

Shaffrey, L. C., et al. (2009), U.K. HiGEM: The New U.K. high-resolution global environment model—Model description and basic evaluation, *J. Clim.*, *22*(8), 1861–1896.

Sime, L. C., K. E. Kohfeld, C. Le Quéré, E. W. Wolff, A. M. de Boer, R. M. Graham, and L. Bopp (2013), Southern hemisphere westerly wind changes during the last glacial maximum: Model-data comparison, *Quat. Sci. Rev.*, *64*, 104–120.

Small, R. J., S. P. deSzoeke, S. P. Xie, L. O'Neill, H. Seo, Q. Song, P. Cornillon, M. Spall, and S. Minobe (2008), Air–sea interaction over ocean fronts and eddies, *Dyn. Atmos. Oceans*, *45*(3–4), 274–319.

Stramma, L. (1992), The South Indian Ocean current, *J. Phys. Oceanogr.*, *22*(4), 421–430.

Toggweiler, J. R., J. L. Russell, and S. R. Carson (2006), Midlatitude Westerlies, atmospheric CO_2, and climate change during the ice ages, *Paleoceanography*, *21*, PA2005, doi:10.1029/2005PA001154.

Tschumi, T., F. Joos, and P. Parekh (2008), How important are Southern Hemisphere wind changes for low glacial carbon dioxide? A model study, *Paleoceanography*, *23*, PA4208, doi:10.1029/2008PA001592.

van Sebille, E., A. Biastoch, P. J. van Leeuwen, and W. P. M. de Ruijter (2009), A weaker Agulhas Current leads to more Agulhas leakage, *Geophys. Res. Lett.*, *36*, L03601, doi:10.1029/2008GL036614.

Wang, Z., T. Kuhlbrodt, and M. P. Meredith (2011), On the response of the Antarctic Circumpolar Current transport to climate change in coupled climate models, *J. Geophys. Res.*, *116*, C08011, doi:10.1029/2010JC006757.

Weijer, W., W. P. M. De Ruijter, and H. A. Dijkstra (2001), Stability of the Atlantic overturning circulation: Competition between Bering strait freshwater flux and Agulhas heat and salt sources, *J. Phys. Oceanogr.*, *31*(8), 2385–2402.

Weijer, W., W. P. M. De Ruijter, A. Sterl, and S. S. Drijfhout (2002), Response of the Atlantic overturning circulation to South Atlantic sources of buoyancy, *Global Planet. Change*, *34*(3–4), 293–311.

Wells, N. C., and B. A. De Cuevas (1995), Depth-integrated vorticity budget of the Southern Ocean from a general circulation model, *J. Phys. Oceanogr.*, *25*(11), 2569–2582.

Wunsch, C. (2011), The decadal mean ocean circulation and Sverdrup balance, *J. Mar. Res.*, *69*(2–3), 417–434.

Zharkov, V., and D. Nof (2008), Agulhas ring injection into the South Atlantic during glacials and interglacials, *Ocean Sci.*, *4*(3), 223–237.